International Conference on Space Optics—ICSO 2018

Chania, Greece

9–12 October 2018

Edited by Zoran Sodnik, Nikos Karafolas, and Bruno Cugny

Novel gratings for astronomical observations

N. Ebizuka

T. Okamoto

M. Takeda

T. Hosobata

et al.

International Conference on Space Optics — ICSO 2018, edited by Zoran Sodnik, Nikos Karafolas, Bruno Cugny, Proc. of SPIE Vol. 11180, 1118069 · © 2018 ESA and CNES · CCC code: 0277-786X/18/$18 · doi: 10.1117/12.2536144

Novel gratings for astronomical observations

N. Ebizuka*[a], T. Okamoto[a], M. Takeda[a], T. Hosobata[a], Y. Yamagata[a],
M. Sasaki[b], T. Kamizuka[c], I. Tanaka[d], T. Hattori[d], S. Ozaki[d], W. Aoki[d]
[a]RIKEN, 2-1 Hirosawa, Wako, Saitama 351-0198, Japan, [b]Faculty of Engineering,
Toyota Technological Institute, [c] Institute of Astronomy, University of Tokyo,
[d]National Astronomical Observatory of Japan.

ABSTRACT

We introduce novel gratings for next generation instruments of the TMT (Thirty Meter Telescope), the 8.2 m Subaru telescope, other ground-based and space-borne telescopes. The reflector facet transmission (RFT) grating which is a surface relief grating with sawtooth shaped grating lattice of an acute vertex angle, is developed for the WFOS of the TMT. The hybrid grism (direct vision grating) for the MOIRCSof the 8.2m Subaru Telescope is developed as a prototype of the RFT grating. The volume binary grating is developed for a high-dispersion echelle grism of the nuMOIRCS as the first light instrument of the ULTIMATE Subaru. We also developing a silicon grism for the MIMIZUKU of the 6.5m telescope of the University of Tokyo Atacama Observatory in Chile and a quasi-Bragg (QB) immersion grating.

Keywords: Volume grating, Echelle spectroscopy, RCWA, Shaper cutting, MEMS technology

1. INTRODUCTION

According as the aperture of a ground-based telescope is enlarged, and the adaptive optics dose not utilize for the telescope, the volume of an astronomical spectrograph becomes huge. On the other hand, in the case of a space-bone telescope, since diffraction limited observations can be achieved even if the aperture of the telescope is changed, the size of the astronomical spectrograph when the wavelength range and the resolving power are the same, does not change. Nevertheless, the light-gathering power is increased as the aperture size of an astronomical telescope becomes larger, scientists demand high dispersion spectroscopic capability for an observational instrument. However, the limitations on the weight and the volume for the space equipment are extremely strict.

The volume of a spectrograph can be downsized by using a transmission grating because a collimator and imaging lens can be placed nearby the transmission grating as shown on the left panel in Fig. 1. Moreover, since a transmission grating achieves perfect Littrow configuration which incidence and diffraction angle are identical, aberrations such as bending of a slit image can be minimize. As number of pixels of a visible and infrared imaging detector has become large, the echelle spectroscopy is widely used in order to observe simultaneously a wide wavelength range with a large resoling power. The echelle spectrograph in which spectrum is folded on to a photographic plate or a 2-dimensional imaging detector, combines a high-order diffraction grating with a prism or a diffraction grating with low angular dispersion as a cross disperser. In the reasons, a transmission grating of echelle type with large angular dispersion and with high diffraction efficiency is required for an astronomical spectrograph of a large telescope such as the TMT (Thirty Meter telescope), the 8.2m Subaru Telescope [1-7].

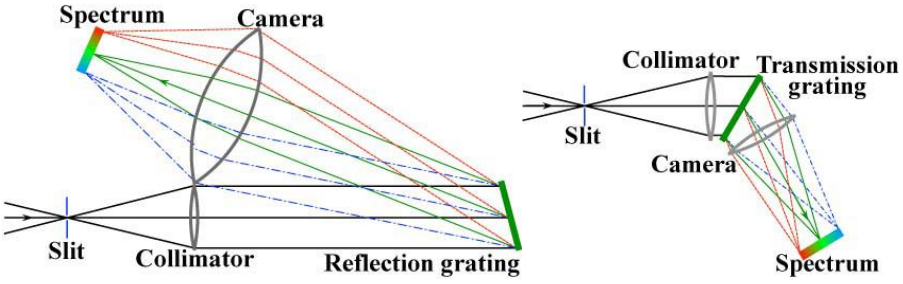

Figure 1 Size of spectrometer of reflactin (upper) and refraction (lower) gratings.

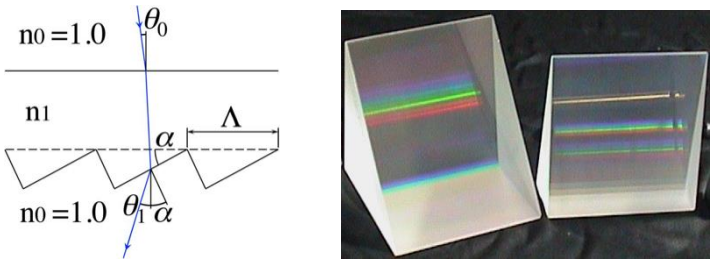

Figure 2 Propagation of incident beam in SR transmission grating with sawtooth shape ridges (left), diffraction efficiency versus lattice period normalized by peek wavelength (middle) [2, 7, 8] and grisms (direct vision grating) for FOCAS (right).

Surface relief (SR) gratings of the transmission type with ridges of the conventional sawtooth shape as shown on the left panel in Fig. 2 are widely used for low dispersion spectrographs. However a SR grating has to increase the refractive index of the ridges as the angular dispersion becomes large due to the limitation of the critical angle. For example, when the incident and the diffraction angles are 45 °, an optical glass and resin are not utilize because the refractive index of the grating ridges needs to be 2.3 or more [1, 2]. On the other hand, a volume phase holographic (VPH) grating, in which the refractive index is modulated sinusoidally, is able to achieve diffraction efficiency up to 100% for S or P polarization at the first diffraction order [8, 9]. VPH gratings are installed in numerous astronomical instruments including the 8.2 m Subaru telescope in order to achieve several times larger angular dispersion as a SR transmission grating [10, 11]. However, since the VPH grating has low diffraction efficiency in higher diffraction orders, it is unsuitable for an echelle spectrograph.

We introduce novel gratings. The reflector facet transmission (RFT) grating [12, 13] is developed for the WFOS (Wide Field Optical Spectrograph) of the TMT [1, 2], hybrid grism (direct vision grating) [12, 13] is developed for the MOIRCS (Multi-Object InfraRed Camera and Spectrograph) of the Subaru Telescope [14], and an echelle grism with a volume binary (VB) grating is developed for the nuMOIRCS of the ULTIMATE Subaru [15]. We also introduce a silicon grism developed for the MIMIZUKU (Mid Infrared Multi-field Imager for gaZing at the UnKnown Universe) of the 6.5m TAO (the University of Tokyo, Atacama Observatory) Telescope in Chili [16] and a quasi-Bragg (QB) immersion grating [12, 17]. The immersion grating has the big advantage for an astronomical spectrograph especially in the infrared wavelength since the size of a spectrograph can be dramatically reduced by using an immersion grating of silicon (n ~ 3.3) or germanium (n ~ 4.0) or a high index material.

2. REFLECTOR FACET TRANSMISSION GRATING

The RFT grating as shown on the left panel in Fig. 3 achieves high diffraction efficiency in large angular dispersion even if the refractive index of is small, since the incident beam is folded in the blaze direction by total reflection on the facet which is opposite to the beam entrance facet [12, 13]. The RFT grating is expected to put into practical use for the WFOS of the TMT, for instruments of ground based and space-borne telescopes. The transmission gratings for the WFOS should be Littrow configuration that is the same incident and diffraction angles of 36~53°, the grating period of 2~5μm, the diffraction orders of 5th~9th or 8th~13rd. We had calculated diffraction efficiency of the RFT grating with the grating period of 5μm, incident and diffraction angles of 45° by using the rigorous coupled wave analysis (RCWA) method [18, 19]. As a result, the RFT grating which height of ridges is 9μm, vertex angle is 38.3°, achieves diffraction efficiency about 80% above 4th diffraction order as shown on the middle and right panels in Fig. 3.

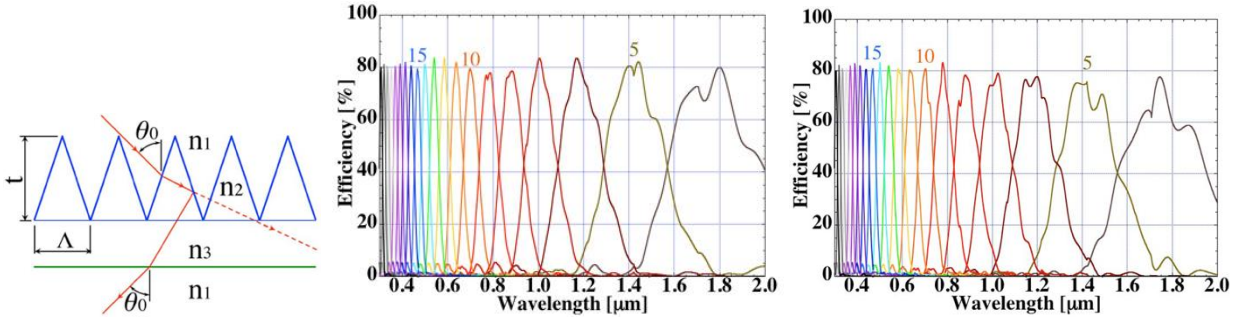

Figure 3 Schematic representation of RFT grating (left), diffraction efficiencies of *S* (middle) and *P* (right) polarization for RFT gratings

with Λ = 5 μm, t = 9 μm, n_1 =1.0, n_2 = n_3 =1.54 and θ_B = 45°.

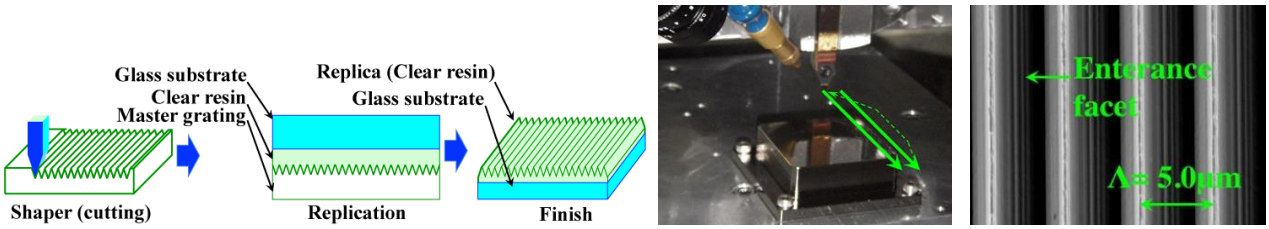

Figure 4 Fabrication process of SR transmission grating (left) [7], fabrication by shaper cutting (middle) and SEM photograph of grating lattice (right) of RFT grating.

As a fabrication method for the RFT grating, a mold of SR grating with acute vertex angle is formed onto a workpiece of an electroless nickel-phosphorous plating by shaper cutting, then a SR transmission grating is replicated from the mold as shown on the left panel in Fig. 4. The mold of the RFT grating was fabricated by shaper cutting method with polycrystal diamond tool (BL-UPC-T, A.L.M.T. Corp.) attached to the ultra-high precision machine (Nagase Integrex Co. Ltd., NIC-M200) of RIKEN as shown on the middle panels in Fig. 4. The mold of the RFT grating of the 1st test fabrication has burrs on edge of the ridges. As a result of the replication, the replica could not remove from the mold. We found a shaper cutting process which is able to form almost ideal ridge shape by the 2nd test fabrication of a mold as shown on the light panels in Fig. 4. We will perform the 3rd test fabrication of a mold for replication tests.

3. HYBRID GRISM

Since the RTF gratings for the WFOS have small vertex angles between 35 and 44 °, it supposed to be difficult in the mold fabrication and the replication processes. Therefore, we decided to fabricate a SR transmission grating with the vertex angle of ridges about 60° for the medium dispersion grism (hybrid grism) of the MOIRCS as a prototype for a RFT grating.

The current medium dispersion grism (R1300 grism) was directly formed ridges onto a prism of soft mixed crystal of TlBr and TlI, so called KRS-5 (n = 2.40@1.65μm), by a ruling engine. However, diffraction efficiency of the R1300 grism had been up to 40% from the beginning, and fine cracks were generated on the surface while repeating the heat cycle between the room temperature and 80 K, and the efficiency further decreased. The hybrid grism instead of the R1300 grism combines a SR transmission grating of replica (n=1.52@ 1.65 μm, grating period: 10.8μm) with a ZnSe prism (n= 2.45@1.65μm, vertex angle: 23.8 °) as shown on the left panel in Fig. 5 [12, 13]. The vertex angle of ridges was 61.8 ° at first designed by geometrical optics as shown in Fig. 5.

A prototype mold with size of 50×50 [mm] for the replica experiments of the hybrid grism was fabricated in RIKEN by shaper cutting with a tool of poly-crystal diamond tool attached to the ultra-high precision machine. The wavefront error is about λ/8@633 nm in RMS (Fig. 6 upper), which is a practical value even for reflection gratings of visible wavelength. The experiments of replication process using the prototype mold were successfully performed in cooperation with Shimadzu Corp. The wavefront error of the replicas of the first and the second generations are about λ/14@633 nm in rms, respectively

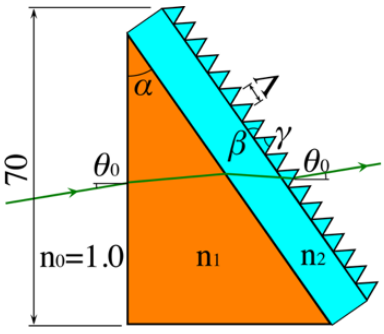

Figure 5 Schematic representation of hybrid grism for MOIRCS.

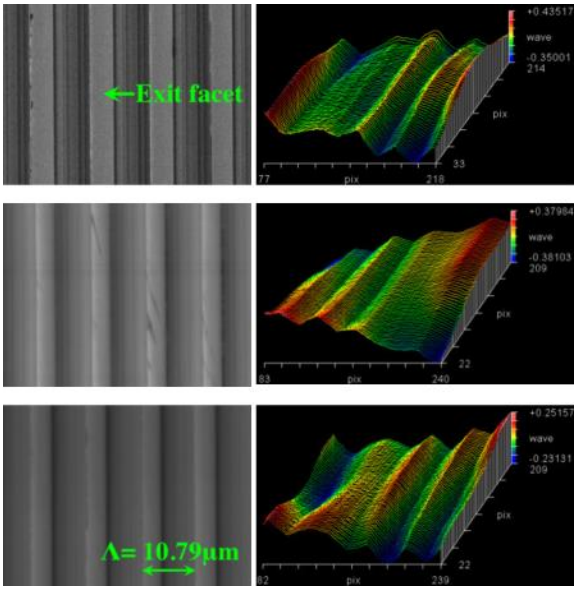

Figure 6 SEM photograph (left) and wave front error right) of MOIRCS hybrid grism. Mold of test fabrication (upper, PV: 0.79λ, RMS: 0.12λ, reflection), replica of 1st generation (middle, PV: 0.76λ, RMS: 0.12λ, transmission), replica of 2nd generation (lower, 0.48λ, RMS: 0.07λ, transmission).

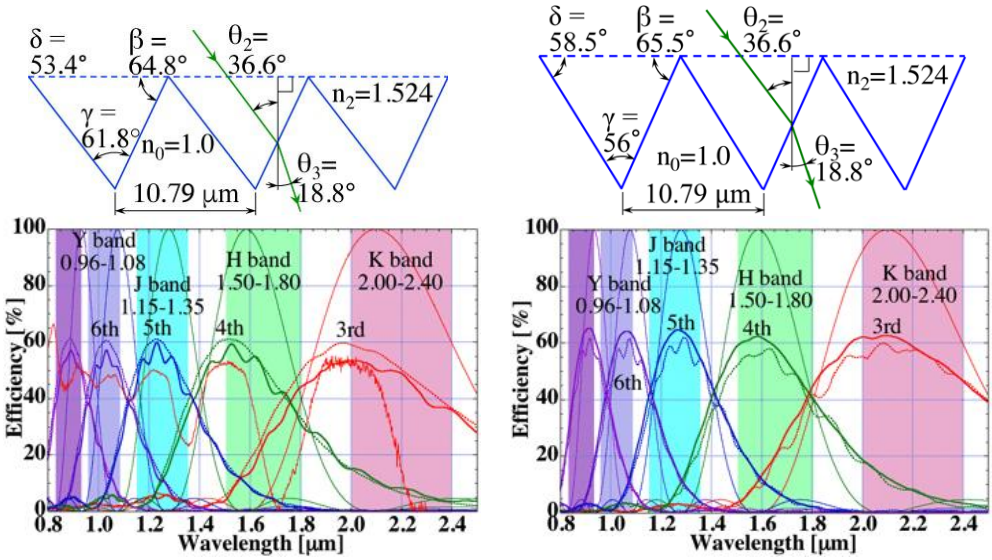

Figure 7 Diffraction efficiency of MOIRCS hybrid grism, left; designed shape, right; improved shape [1].

(Fig. 6 middle and lower). The hybrid grism uses in 0.96 μm or longer wavelength, so the replicas satisfy sufficiently for the specification of the MOIRCS grism.

As a result of measurements of the diffraction efficiency, the peak efficiency of the prototype of the replicated SR transmission grating was about 50-55% (Fig. 7 lower left). The spectral properties of the diffraction efficiency of the replicated grating were investigated by numerical calculations using RCWA (Rigorous coupled-wave analysis) method and it was found that property of the diffraction efficiency is shifted toward the shorter wavelength. Therefore, we sought the optimum spectral properties of the diffraction efficiency of the SR transmission grating by changing the angle of the facet (β) from which the beam exits and the vertex angle (γ) of the ridges. As a result, we found that the spectral property and the diffraction efficiency are optimum (Fig. 6 lower right) when the shape of ridges is β=65.5° and γ=55.0° as shown on the upper right in Fig. 6.

4. ECHELLE GRISM

The nuMOIRCS is scheduled as the first light instrument for the ULTIMATE Subaru. The ULTIMATE Subaru plans to install a new ground-layer adaptive optics (GLAO) onto the Subaru telescope. The GLAO improves the limiting magnitude and the spatial resolution by reducing the size of the star image by correcting the wavefront error due to the atmospheric turbulences. The echelle grism for the spectrum from the third to the sixth diffraction orders installs in the nuMOIRCS. The echelle grism combined with a direct vision prism as a cross disperser can simultaneously covert the wavelength range of 0.8 to 1.8μm with large angular dispersion by folding the spectra onto the detector, and it is the key optical element to improve performance of the nuMOIRCS.

The VB grating uses the total reflection by a low-index medium as the mirror surface as shown on the left panel in figure

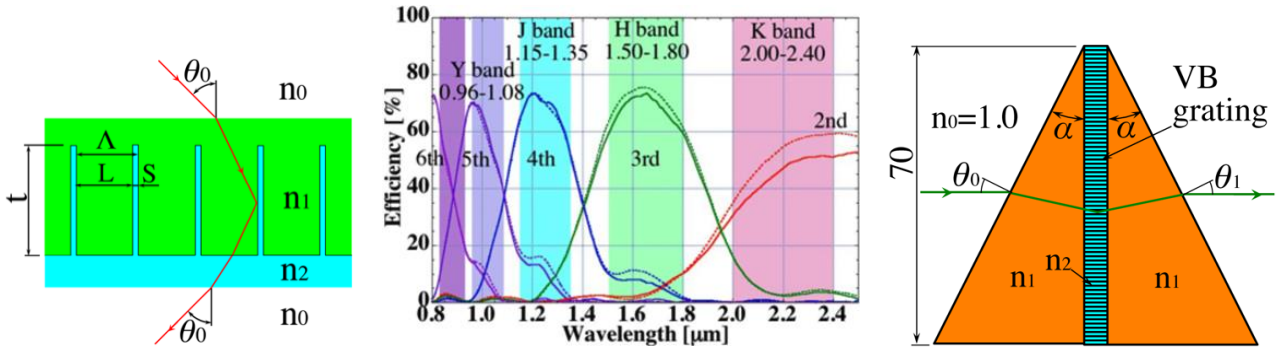

Figure 8 Schematic representation of VB grating (left), diffraction efficiency of VB grating for echelle grism of nu-MOIRCS (middle: θ_0=28.4°, n_1=1.33, n_2 = n_3 =1.6, Λ= 5.1 μm, L&S = 4.6:0.5 [μm], t = 16 μm), and echelle grism (right).

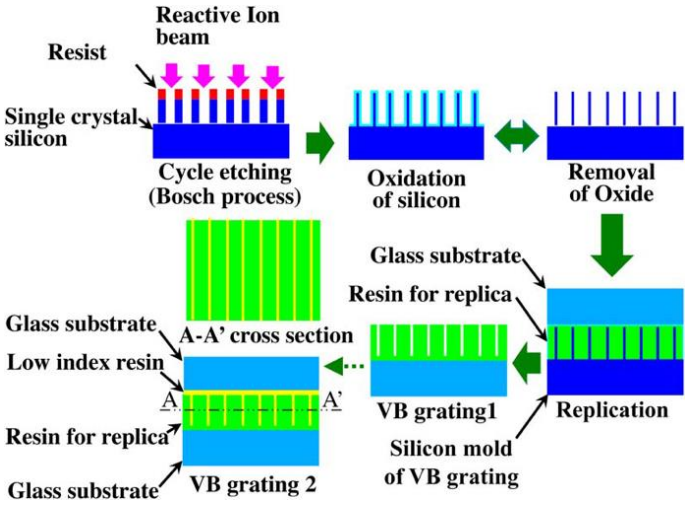

Figure 9 Fabrication process for VB grating by using silicon mold.

8. We found that higher diffraction efficiencies can be achieved by the VB grating (lattice period Λ=5.1μm, L & S=4.6: 0.5 [μm], thickness t=16μm) for the echelle grism by numerical calculations using the RCWA method as shown on the right panel in figure 8 [12, 13, 20]. We decided to develop a VB grating for the echelle grism of the nu-MOIRCS. The echelle grism is fabricated by sandwiched the VB grating between two ZnSe prisms as shown on the middle panel in figure 8.

We develop a fabrication method for a VB grating as a mold of silicon with ridges of high aspect ratio in Toyoda Institute of Technology. By numerous trial fabrications, we found the process as shown in Fig. 9 which oxygen is slightly added to the etching gas and the passivation gas, cleaning is performed while etching and sidewall protection (Bosch process), and the amount of an etching volume is reduced. As a result, the scallops (irregularities formed every etching cycle) on the sidewall of the ridges successfully reduced to about 40 nm. Further, silicon oxide layers are formed on both sides of the ridge (sidewalls) surfaces of the silicon, and then the oxide layers are etched. By repeating this process several times, it was possible to obtain extremely smooth surfaces with little scattering even in visible light. Specifically, a resist was formed on a silicon substrate by using a mask with a line & space of 2.0μm: 3.1μm. Deep grooves formed by the cycle etching onto the silicon substrates (two kind of depths with 10μm and 20μm). Silicon oxide layers are formed and removed twice. Where oxygen diffuses from a surface of the silicon is about 400 nm by the oxidation process when an oxide layer having a thickness of about 1μm. As a result, lattices of ridges with widths of 0.44 and 0.8 μm, respectively, which surfaces are extremely smooth, are obtained (Fig. 10 left and middle). The silicon VB grating with tapered grating lattice on the right panel in Fig. 10 is suitable for mold. Although the etching and sidewall protection process of the tapered VB grating are almost the same as the other VB gratings in Fig. 10, applied voltage or gas pressure is slightly different. We are performing replication tests by using the tapered VB grating.

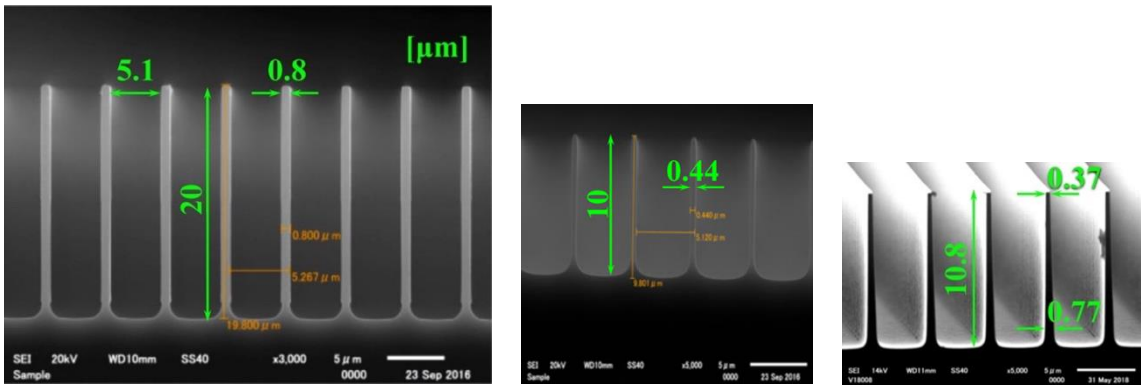

Figure 10 Silicon VB grating as a mold.

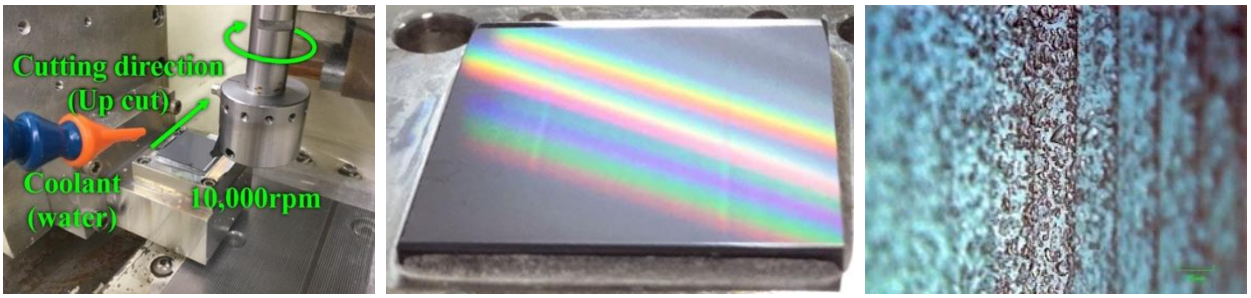

Figure 11 Fabrication of Si grism grating by fly cutting (left), Si grism for MIMIZUKU (middle) and microscope photograph of grooves (right).

5. GRISM FOR NEAR TO MID INFRARED

We are developing a silicon grism with a grating lattice of sawtooth shape for the near to mid-infrared channel of the MIMIZUKU. The MIMIZUKU of the TAO Telescope has near to mid-infrared (2~5.3μm), mid-infrared (6.8~26μm) and mid to far infrared (24~38 μm) channels [16]. After several trial fabrications, we performed trial fabrication of silicon grism (24×24×t2.8, apex angle: 4.2°) by means of fly-cutting with a single-crystal diamond tool (UPC-T tool, A.L.M.T. Corp.) attached to an ultra-high precision machine (Toshiba Machine Co. Ltd., ULG-100A) in the last year (Fig. 11 left). However, diffraction efficiency of the grism is about 5% because the grating lattice was rough surface (Fig. 11 middle and right). We are planning to fabricate a germanium grism instead of the silicon grism in this year.

6. QUASI-BRAGG IMMERSION GRATING

An immersion grating is a reflection grating filled with a high-refractive index medium in its optical path, and angular dispersion of the immersion grating is proportional to the refractive index of the medium [21, 22]. In other words, since the size of an immersion grating can be reduced in inverse proportion to the refractive index of the medium compared with a conventional reflection grating with the same angular dispersion.

The Quasi-Bragg (QB) immersion grating [12,17] was fabricated by combination of an inclined QB grating, Littrow prism (22 x 22 x 38.1 mm) and surface reflection mirror as shown on the left and middle in figure 12. The block of 60 seats of silica substrates with 0.5 mm in thickness was stacked by room temperature bonding of gold in Tohoku University [23]. The QB grating was cut with inclination of 30° from the block of silica substrates. We assembled a spectroscopic optical system of the Littrow mount (angle between incident and diffracted beams is small), and observed a diffraction image of the QB immersion grating using a He-Ne laser as a light source. As a result, although the order could not be separated because the point source image of the pinhole was larger than the interval of the diffraction orders, the diffraction intensity was highly concentrated (blazed) as shown on the right panel in figure 12, we confirmed the QB immersion grating functions as an immersion grating. It is difficult to fabricate a QB immersion grating for visible to near infrared wavelength by lamination of mirror substrates. On the other hand, it is relatively easy to fabricate a QB immersion grating of silicon or germanium for mid and far infrared wavelength by the lamination of mirror substrates.

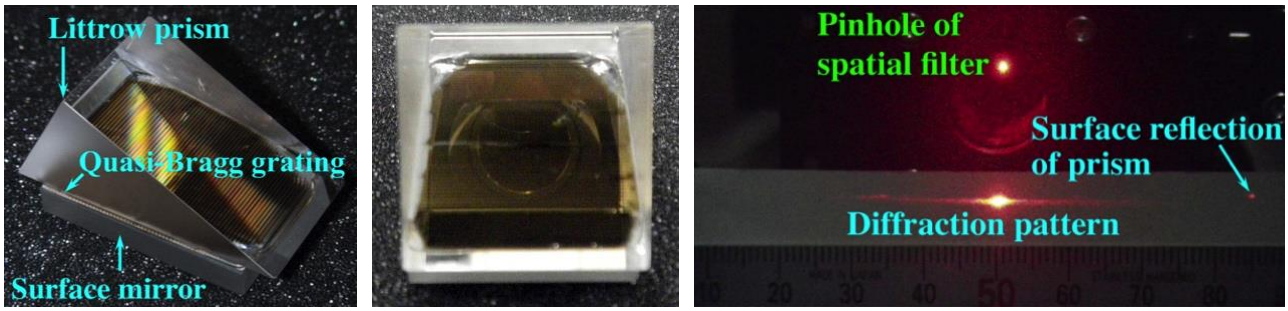

Figure 12 Prototype of QB immersion grating (left), camera lens image of diffraction beam gazed from square surface of Littrow prism (middle) and diffraction pattern of QB immersion grating (right).

7. CONCLUSIONS

The RFT grating and the VB grating which function as transmission gratings at high diffraction orders are able to achieve high diffraction efficiency. The mold of the SR grating for the hybrid grism of the MOIRCS as a prototype of the RFT grating was produced by diamond cutting process. As a mold for the VB grating of the echelle grism of the nuMOIRCS, we succeeded in prototyping a silicon grating mold with the grating lattice of a high aspect ratio. Fabrication of a silicon grism for the MIMIZUKU was failed. We are planning to fabricate a germanium grism for the MIMIZUKU. The QB immersion grating was fabricated by combination of a QB grating inclined at 30 degrees, Littrow prism and a surface reflection mirror. We confirmed the QB immersion grating functions as an immersion grating.

We will fabricate a mold for the replication experiment (size: 50 × 50 [mm]) of RFT grating (vertex angle 38.3 °) and a mold of the SR grating (vertex angle 56 °) for the actual hybrid grism (size: 70 × 70 [mm]) of the MOIRCS by shaper cutting process. The VB grating for the echelle grism of the nuMOIRCS with high dispersion will continue to be promoted through collaborative research with Toyoda Institute of Technology. In addition, we plan to prototype a germanium grism of near-mid infrared for MIMIZUKU by fly cutting process.

We appreciate Mr. Keizo Kajiura, Mr. Ken Kajiwara and Mr. Toshio Okumura of Nanotechnology Platform facilities, the Toyota Institute of Technology for their assistance on the trial fabrications of the VB gratings. Dr. Uomoto and Prof. Shimatsu of Tohoku University performed the room temperature bonding of gold for QB grating fabrications. We utilize facility of the Advanced Technology Center of National Astronomical Observatory of Japan (NAOJ) for grating measurements and "Nanotechnology Platform Japan" of the Ministry of Education, Culture, Sports, Science and Technology (MEXT), Japan for grating fabrications. This work is supported by the grant-in-aid of NAOJ for TMT strategic basic research and development, by the Grant-in-Aid for Challenging Exploratory Research, 2015-2016, 15K13470; from MEXT. And this work was supported by the grant-in-aid of NAOJ for Joint development research, and by Adaptable and Seamless Technology Transfer Program through Target-driven R&D, 2013-2014, from Japan Science and Technology Agency.

REFERENCES

[1] Simard, N.L., et al., "The instrumentation program for the Thirty Meter Telescope," Proc. SPIE **8446**, 1F, (2012).
[2] Kevin. B., et al., "WFOS instrument trade study: slicer vs. fiber instrument concept designs and results," Proc. SPIE **10702**, 20 (2018).
[3] Minowa, Y., *et al.*, "An overview of current and future instrumentation at the Subaru telescope," Proc. SPIE **9908**, 06 (2016).
[4] Ramsay, S. K., *et al.*, "The E-ELT instrument roadmap: a status report," Proc. SPIE **9147**, 1Z (2014).
[5] Pasquini, L. and Hubin, N, "The ESO Paranal Instrumentation Programme," Proc. SPIE **10702**, 04 (2018).
[6] Jacoby, G. H., *et al.*, "Instrumentation Progress at the Giant Magellan Telescope Project," Proc. SPIE **9908**, 1U (2016).
[7] Roelfsema, P. R., *et al.*, "SPICA: a joint infrared space observatory," Proc. SPIE **10698**, 0A (2018).
[8] Barden, S.C., Arns; J.A. and Colburn, W.S., "Volume-phase holographic gratings and their potential for astronomical applications," Proc. SPIE **3355**, 866-876 (1998).
[9] Baldry, I. K., Bland-Hawthorn, J. and Robertson, J. G., "Volume Phase Holographic gratings: Polarization properties and Diffraction Efficiency," PASP **116,** 403-414 **(**2004).
[10] Ebizuka, N., et al., "Cryogenic VPH Grisms for MOIRCS," PASJ **63**, S605-S612 (2011).
[11] Ebizuka, N., et al., "Grisms Developed for FOCAS," PASJ **63,** S613-S622 (2011).
[12] Ebizuka, N., et al., "Novel gratings for next generation instruments of astronomical observations," Proc. SPIE **9912**, 0M (2017).
[13] Ebizuka, N., et al., "Novel diffraction gratings for next generation Spectrographs with high spectral dispersion," Proc. SPIE **9912**, 2Z01-2Z10 (2016).
[14] Ichikawa, T., et al., "MOIRCS: multi-object infrared camera and spectrograph for SUBARU," Proc. SPIE **6269**, 16 (2006).
[15] Hayano, Y., et al., "ULTIMATE-SUBARU: project status," Proc. SPIE **9148**, 2S01-2S08 (2014).
[16] Kamizuka, T., *et al*., "Development status of the mid-infrared two-field camera and spectrograph MIMIZUKU for the TAO 6.5-m Telescope," *Proc. SPIE* **9908**, 3W (2016).

[17] Ebizuka, N., et al., "Birefringence Bragg Binary (3B) Grating, Quasi-Bragg Grating and Immersion Gratings," Proc. SPIE **9151**, 5C1-5C9 (2014).
[18] Moharam, M. G. and Gaylord, T. K., "Rigorous coupled-wave analysis of planar-grating diffraction," JOSA **71**, 811 (1981).
[19] Li, L., "Note on the S-matrix propagation algorithm," JOSA **A 20**, 655 (2003).
[20] Bianco, A. and Ebizuka, N., "Echelle VPHG: a step forward," Proc. SPIE **8450**, 431-438 (2012).
[21] Larsson, T and Neuhaus, "The Immersion Grating: Spectroscopic Advantages and Resemblance to the Echelon Grating" Zeitschrift fr Naturforschung A **23**, 2130-2032 (1968).
[22] Wiedemann, G. and Jennings, D.E., "Immersion grating for infrared astronomy", Appl. Opt. **32**, 1176-1178, 1993
[23] Shimatsu, T. and Uomoto, M., "Room Temperature Bonding of Wafers with Thin Nanocrystalline Metal Films," ECS Transactions **33**, 61-72 (2010).

[24] Uehara, M., *et al*., "Development of the Wide Field Grism Spectrograph 2," Proc. SPIE **5492**, 661-668 (2004).
[25] Watanabe, M., *et al*., "TRISPEC: A Simultaneous Optical and Near-Infrared Imager, Spectrograph, and Polarimeter, " PASP **117**, 870-884 (2005).
[26] Oka, K., et al., "Optimization of a volume phase holographic grism for astronomical observation using the Photopolymer," Proc. SPIE **5005**, 8-19 (2003).
[27] Oka, K.; Ebizuka, N. and Kodate, K., "Optimal design of the grating with reflective plate of comb type for astronomical observation using RCWA," Proc. SPIE **5290**, 168-178 (2004).
[28] Gupta, M. C. and Peng, S. T., "Diffraction characteristics of surface-relief gratings," Appl. Opt. **32**, 2911-2917 (1993).
[29] Gerritsen, H. J. and Jepsen, M. L., "Rectangular surface-relief transmission gratings with a very large first- order diffraction efficiency (95%) for unpolarized light," Appl. Opt. **37**, 5823-5829 (1998).